Effect of time of microwave activation synthesis on crystallite size of spheroid β Tricalcium Phosphate nanopowders

Z. Gandou [1,2], A. Nounah [1], K. Nouneh [3], A. Yahyaoui[4]

[1]*Mohammed V University, High School of Technology, Laboratory of materials and environment , Avenue Prince Héritier, B.P.227, Salé, Morocco*

[2]*CNESTEN, Laboratory of Inorganic Chemistry synthesis, Laboratory of structural and isotopiques analysis, laboratory exploitation Department, Rabat BP 1382 Rabat Principal*

[3]*Ibn Tofail University, Laboratory of Physics of condensed Matter Physics Department, Kenitra Morocco*

[4]*Mohammed V Agdal University, Faculty of Sciences, Laboratory of Radiochemistry and Nuclear Chemistry, B.P. 1014 RP, Rabat, Morocco*

Abstract

βTricalcium phosphate nanopowders was successfully synthesized by the microwave activated co-precipitation in ambient atmospheric method without adding any surfactant. The synthesized were calcined at 900°C to obtain monophasic βTCP. The powder were characterized using X-ray diffraction, Fourier Transform-Infrared spectroscopy (FT-IR),and transmission electron microscopy to study structure and stability of product as synthesized and after calcination at 900°C. The results showed that amourphous calcium phosphates (ACP) and calcium deficient hydroxyapatite (CDHA) had been synthesized in a rapid way using microwave assisted co precipitation, which was an important processing method introduced to the synthesis of βTCP after calcination at 900 °C. The effects of microwave irradiation, time of irradiation on the reaction mechanism were studied. By using microwave as an assisted method for activation the reaction, the powders can be produced faster by employing an improved and efficient heat transfer throughout the volume and to synthesize nanostructured materials **.** Biocompatible βTCP nanopowders were synthesized with controlled particle size, morphology by this way.

Keywords: spheroid, microwave, ACP, Hap (Hydroxyapatite), βTCP (βTricalcium phosphates)

1 Introduction:

In the latest years, researchers chose to develop and optimize new methods processing of materials with precise control over the crystallographic, chemical structure, controlled size and morphology. The surface properties of the implant play a crucial role to improve both the biological response to implant, the material response to implants and to reacts with the physiological conditions [1-7].

Calcium phosphates (CaP) exhibit excellent biocompatibility and show osteoconductive properties [8-12]. Recently, it was found that β tricalcium phosphate (βTCP) is a good tissue engineering scaffold material in biomedical field because its high capacity of resorption, this type of material presents an excellent biocompatibility and bioactivity while it contacts bone cells as some advantages including the gradual degradation in organisms metabolic process, the stage of replacement and growth of new bone, without prejudice to newly grown bone in material substitution steps and builds a direct chemical connection between bone tissues and ceramics implant   However, applications of βTCP are restricted to relatively small bone defects. Moreover, researchers have shown that nanoscales features improve cell-material interactions in different materials [13, 14].

βTCP nanopowder with different morphology can be used directly in drug or bimolecular delivery applications or can be used for processing nanograin compacts for bone grafts. Bioresorbability of βTCP nanopowder can be

tailored by varying particle size, morphology, surface area, and crystallinity [15]. βTCP cannot be precipitated from aqueous solutions. It is a high temperature phase, which can be prepared at temperatures above 750°C by thermal decomposition of calcium deficient hydroxyapatite CDHA [16, 17].

Numerous synthesis methodologies of calcium phosphates powders are known, such as precipitation, solid state synthesis, hydrolysis, hydrothermal, sol–gel methods and flame synthesis.. The preparation of calcium phosphate ceramics by conventional wet, dry and hydrothermal routes is tedious and time-consuming. Ultrasonic treatment has been used to accelerate the formation of Hap [17].

The microwave synthetic routes have been reported for the preparation nanosize powders of pure or biphasic calcium phosphates within a shorter period of time [18-22]. Microwave synthesis of materials offers the advantages of heating throughout the volume and very efficient transformation of energy. In contrast to the conventional procedures, where the material is externally heated through conduction, microwave heating involves in situ conversion of microwave energy into heat using the inherent properties of reaction mixture [23–25]. Reaction times are shorter than those required conventionally producing samples having comparable X-ray powder patterns with a specific morphology (table 1).

2. Experimental

2.1. *Synthesis of calcium phosphate powders*

ACP and CDHA was prepared by co-precipitation of calcium hydroxide $Ca(OH)_2$ and phosphoric acid (H_3PO_4) , as Ca and P precursors, respectively. To form a reaction mixture, 0.45M of H_3PO_4 aqueous solution was added to 0.75M of $Ca(OH)_2$ aqueous suspension under a constant stirring condition at room temperature. In this study, commercially supplied $Ca(OH)_2$ (99.8% purity) and (H_3PO_4) (85.0–87.0%) and the double distilled de-ionized water were the only starting materials. The powders were synthesized at a fixed Ca/P molar ratio of 1.5.

The mixture as prepared was immediately exposed to microwave radiation (850 W) for 11 minutes interspersed with samples taken after 5, 3, 2 and 1 minutes of heating. A white paste subsequently is formed. The times of heating by microwave are the following: Time (mn) t_1 = 5 mn (Hap5), t_2 =8 mn (Hap8); t_3 = 10 mn (Hap10); t_4= 11mn (Hap11)
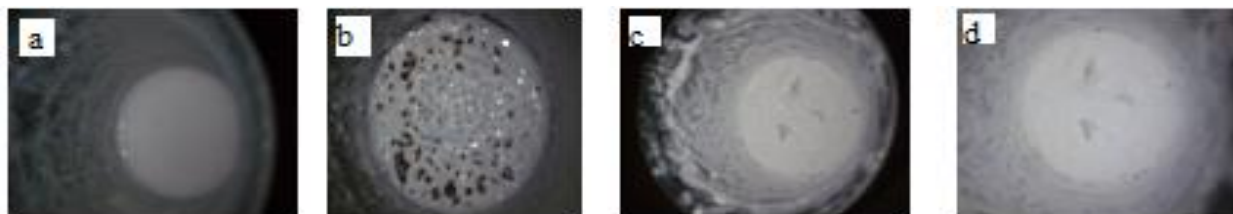

Figure 1: Steps of synthesis of calcium phosphates by microwave activation (a = Hap5, b = Hap8, c = Hap10, d = Hap11)

The pastes resulting from this treatment are maintened for 36 hours at a temperature of 37°C.

These powders were then calcined at 900 °C and holding for 1 h to increase their crystallinities. The calcined samples are Hapc5, Hapc8, Hapc10 and Hapc11.

2.2 *Characterization of calcium phosphates :*

The physical and chemical analyses were carried out on the dried precipitate and the powder annealed at 900 °C. The phases formed were identified by the time heating in microwave as dried and after heating,

2.2.1. *XRD analysis :*

Crystalline phases were identified (Theta/Theta) X-ray diffractometer (XRD) (SIEMENS D5000, λCu=1.5408 Å). XRD patterns were collected over the 2θ range of 0-90°. The software used for data processing of X-ray diffraction was DIFFRACT/AT. Crystalline phases detected in the patterns were identified by comparison to the standard patterns From the ICDD/PDF (International Center for Diffraction Data-Powder Diffraction Files).

2.2.2 *FTIR measurements:*

The Fourier transform infrared spectra (FTIR) were obtained by infrared spectroscopy (Nicolet AVATAR 360)with the wave numbers recorded from 400 to 4000 cm^{-1} at 2 cm^{-1} resolution. small amount of sample powders was blended with KBr and then pressed into discs for the measurement.

Table1 shows Different methods to synthesize calcium phosphates by microwave

Starting materials	Template additives	Nature of microwave	Power	time	pH	Authors And Ref	Outcome powder morphology and property
$Ca(CH_3COO)_2$, Na_2HPO_4, NaH_2PO_4	Sodium citrate HCl	Professional Microwave Autoclave	120°C	30min	5	Wang 2011 [26]	Hap microsphere from 0.5 to 2 µm and exhibit three-dimensional nanoporous network structure.
$Ca(NO_3)_2x4H_2O$ KH_2PO_4	NH_4OH	1Ultrasonic 2 Commercial microwave	50 W 1100W	1 h -	9	G.E.J. Poinern et al 2011 [27]	Uniform Spherical particles with size from 40 to 50 in diameter.
	HNO_3 $NaNO_3$	Microwave oven	600 W	5 min	_	Sahil jalota et al 2004 [28]	Monodispersed nanowhiskzers of Hap with 1 µm and 100 nm Ion substitution cause deviation of stochiometry
$Ca(NO_3)_2x4H_2O$ / $(NH_4)_2HPO_4$	NH_4OH	Sonochemistry-assisted microwave reactor with reflux cooling	180 W 200 W	10 min ,30 min	10,5	Tong Liang et al 2013 [29]	Uniform rod like nanoparticles with different dimension (diameters and length : 50°C : d 15 nm L: 40 nm 90°C d: 30 nm L : 100 nm At 10°C : flake like morphology without mesoporous structure
	CTAB in alcool/water NH_4OH	Domestic microwave with refluxing	1000W	3min	9	Rabia Nazir et al 2013 [30]	βTCP spherical morphology 50 à 80 nm
	NH_4OH	Domestic microwave with refluxing	600W 850W 1000W	1 min 3min 5min 10	10	Rabia Nazir et al 2011 **[31]**	Hap spherulites agglomerates with narrow size distribution around 0, 80 µm
	NH_4OH	Professional Microwave	50°C	40 min	7	Li Sha et al 2011 [32]	Pur βTCP short rod-like with the size of 80–150 nm in width and 200–300 nm in length.
$Ca(NO_3)_2x4H_2O$ Na_2HPO_4	EDTA	Domestic Microwave with Refluxing	600W	19 min 3 min ON 5 min OFF	9	S.J.Kalita S.Verma 2010 [33]	Highly crystalline powder of 10 nm-50 nm Rod shaped 5 nm in diameter and 15 nm in length elliptical: 16 nm x 27 nm
	CTAB NaOH	Microwave	900W 2.45 GHz	5 min		Arami 2009 [34]	Hap nanostrips with average width and length of 10 and 55 nm, respectively
$Ca_3(NO_4)_2x4H_2O$ H_3PO_4	wihout	Domestic microwave	175W 525W 660 W			Sidharthan 2005 [35]	Needle shape 39-56 nm length, 12-14 nm width Acicular shape; 10-16 nm length, 10-12 nm width Platelet shape; 32-42 nm length, 12-25 nm width
	1,2 Ethylendiamine	Microwave Hydrothermal Max 1200 W	100 °C 120 °C 140 °C	3 min	_	Y.Z.Wang et al 2011 [36]	Pure nano crystalline calcium deficient Hap Crystallinity degree, crystallite size and morphology of powder change with temperature and/or time. 54,7 nm (140°C for 1 min)
$(NH_4)_2HPO_4$ $Ca(OH)_2$	NH_4OH NaOH	Domestic microwave	900 W	30,45,60, 75,90,120 min	≥ 9	RAMLI et al 2012 [37]	Needle shaped particles with length ranging 80-100nm and with around 10-15 min
		Domestic microwave	1100W	30 min	11	Rameshbabu et al 2009 [38]	Nanostructured biphasic calcium phosphates with crystallite size using sheerer formula 20 nm 24 nm
	$CaCO_3$ $MgCO_3$	Domestic microwave	800W	40 à 45 min	_	Kumar et al 2000 [39]	To form biphasic calcium phosphate mimicking one resorption by varying the amount of carbonate ion
	without	Precipitation mw	850W	20 min	≥ 10	Meejoo et al 2006 [18]	Needle shape; 50 nm diameter, 200 nm length 28-159 nm particle size
$Ca(OH)_2$ / H_3PO_4	without	Domestic microwave Acide base	850W	11 min		This study	Spherical Nano TCP calcium phosphate with serious agglomerate
	HNO_3 NaOH	Domestic microwave Acide base	800W	45 min	9	Ghomach et al 2012 [40]	Spherical Nano Hap-TCP biphasic calcium phosphate with serious agglomerate
	HNO_3 NaOH	Domestic microwave Acide base	800W	45 min	6,8,9 ,10	Farzadi 2011 [41]	Hap/ βTCP grain size of powders 43 to 55 nm and the grain size of powders produced by acid-base
	without	Domestic microwave Acide base	700W	25 min	6,81 0,12	Lee et al 2007 [42]	Hap and biphasic TCP nanopowder with spherical shape pH 6 : 80 – 90 nm pH 12 : 50 – 70. The ratio Hap/TCP and particles size change with Ph

2.2.3 *Thermogravimetric analysis :*

Thermogravimetric analysis (TGA) were conducted under air using a TA Instruments Q500 apparatus with 10°C min^{-1} ramp between 25 and 1000°C. Mass losses in TGA plot represent thermal stability of the sample and may also represent chemical decomposition or vaporization and sublimation at higher temperatures.

2.2.4 *TEM analysis :*

The size of nanoparticles was performed by a Tecnai G2 microscope at 120 Kv in dark field.

3. Results and discussion:

3.1 *XRD analysis*

The XRD patterns of samples before and after calcinations are shown in figure 2 and 3 respectively. The as dried sample Hap5 show a single broad peak around 2Ɵ = 32° identified as Amorphous Calcium Phosphate (ACP), revealing their amorphous nature. The Hap8, Hap10 and Hap11 can be indexed as CDHA phase according to the standard pattern (JCPDS N° 09-432). This result confirms the further characterization with FTIR also confirms the formation of CDHA.
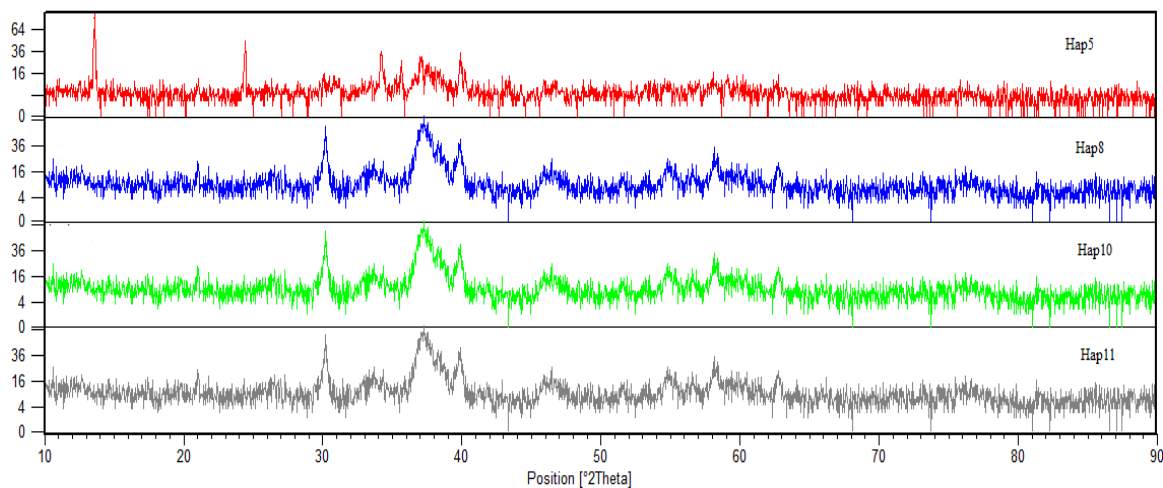

Figure 2: XRD analysis of the effect of time of microwave activation on nanocrystalline apatites

On the other hand, we can see in figure 3 that the Hapc5 sample demonstrated some weak diffraction peaks that match those of standard (JCPDS N° 09-432), but for other samples Hapc8, Hapc10 and Hapc11, the peaks were identified to be corresponding to βTCP and indexed according to the standard value (JCPDS 09-0169).
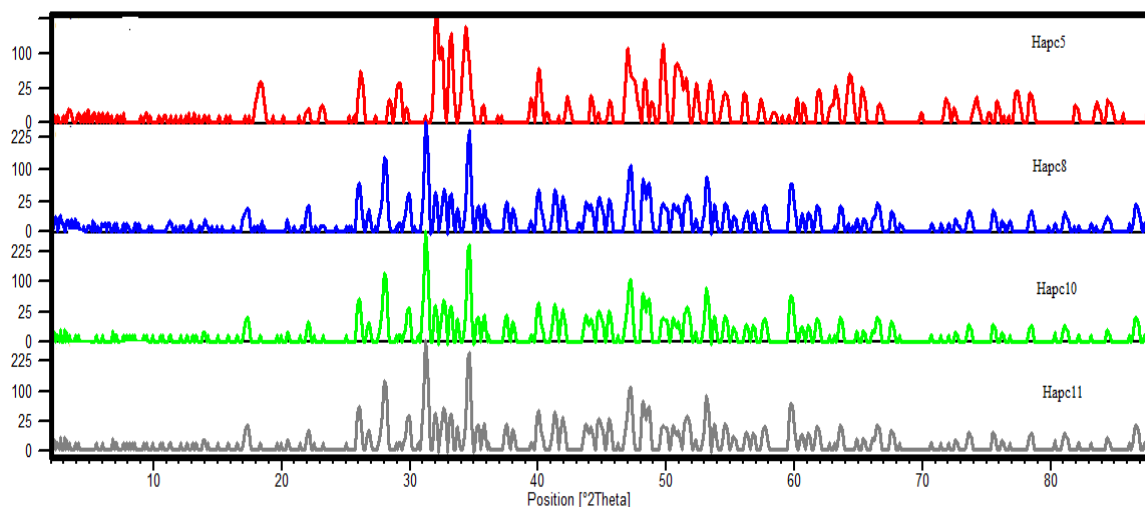

Figure 3: XRD analysis of the effect of time of calcination on nanocrystalline apatites

3.2 *Infra red analysis :*

The FTIR spectra of the as obtained powders at Hap8, Hap10 and Hap11 display the similar profile in figure 1. As listed in table 2, the hydroxyl OH^- bond stretch at around (633 and 3440 cm^{-1}) prove presence of Hap **[43]**, PO_4^{3-} (472, 563, 602, 961, and (1035-1089 cm^{-1}) , and residual H_2O (3431 and 1640 cm^{-1}) whereas the weak bands. Absorption bands 873 cm^{-1} 1425, 1455 can be attributed to HPO_4^{-2} substitutes phosphate ion, revealing that B- type carbonate Hap is formed [43-44]. By the presence of HPO_4^{-2} ions bands the spectra exhibit clear evidence of CDHA [45-47]. The CDHA also exhibit low intense OH^- stretching and librationals modes than stochiometric Hap [48].

After calcinations at 900°C, the disappearance of the hydroxyl OH^- bands and carbonate CO_3^{2-} band has been noticed for all samples except sample of Hap5. The presence of new bands at 1120, 971, and 944 cm^{-1} can be assigned to PO_4^{3-} groups of βTCP [47] (Fig.2). From literature this band can be associated with Ca-deficient apatite (CDAp) after thermal treatment decomposition of CDAp lead to formation of β tricalcium phosphate (βTCP) or biphasic calcium phosphates (BCP) [18-38-49]. For sample Hap5, there is formation of CDHA from intermediate product ACP after calcinations with a small amount of carbonate (CO_3^{2-}) substitution [5].

The results also confirmed that the Hap phase obtained in this work is calcium deficient Hydroxyapatite (CDHA).All CDHA samples showed broad bands corresponding to absorbed water. This may arise due to nanoparticles nature and associated porosities resulting in adsorbed water peak at higher temperature [5].

Table 2: Assignments of infrared frequencies (cm^{-1}) of as synthesized CDHA and heat treated samples

	Infrared frequencies (cm^{-1})							
	As synthesized				After Calcination 900°C			
Assignments	Hap5	Hap8	Hap10	Hap11	Hapc5	Hapc8	Hapc10	Hapc11
PO_4^{3-} bend υ2	472	468	472	466	472	478	472	466
PO_4^{3-} bend υ4	563	563	563	562	569	553	553	551
PO_4^{3-} bend υ4	602	602	600	602	602	604	604	604
Structural OH^-	_	632	633	633	632	_	_	_
HPO_4^{-2}	873	873	873	873	873	_	_	_
PO_4^{3-} stretch υ1	961	962	961	961	962	_	_	_
PO_4^{3-} stretch υ1	_	_	_	_	_	971	970	971
PO_4^{3-} bend υ3	1035	1029	1066	1042	1043	1043	1042	1042
HPO_4^{-2}	1088	1089	1089	1089	1089	_	_	_
PO_4^{3-} bend υ3	_	_	_	_	_	1118	1117	1120
CO_3^{2-} υ3	1420	1425	1425	1425	1413	_	_	_
CO_3^{2-} υ3	1455	1455	1455	1455	1458	_	_	_
H_2O adsorbed υ2	1641	1640	1642	1640	1640	1640	1642	1642
H_2O adsorbed	3441	3439	3438	3431	3571	_	_	_
Structural OH^-	3568	3568	3568	3568	3570	_	_	_

The FTIR spectrum of Hap8, Hap10, Hap11 powders show in figure 5 are similar of characteristics bands of βTCP , the characteristic PO_4^{3-} absorption bands of βTCP, The band at 900-1200 cm^{-1} were the stretching mode of PO_4^{3-} group. The sharp peaks at 552 and 606 cm^{-1} represent the vibration peaks of PO_4^{3-} in βTCP. The absence of sharp peak at 3571 cm^{-1} indicating the absence of OH functional group in the sample.
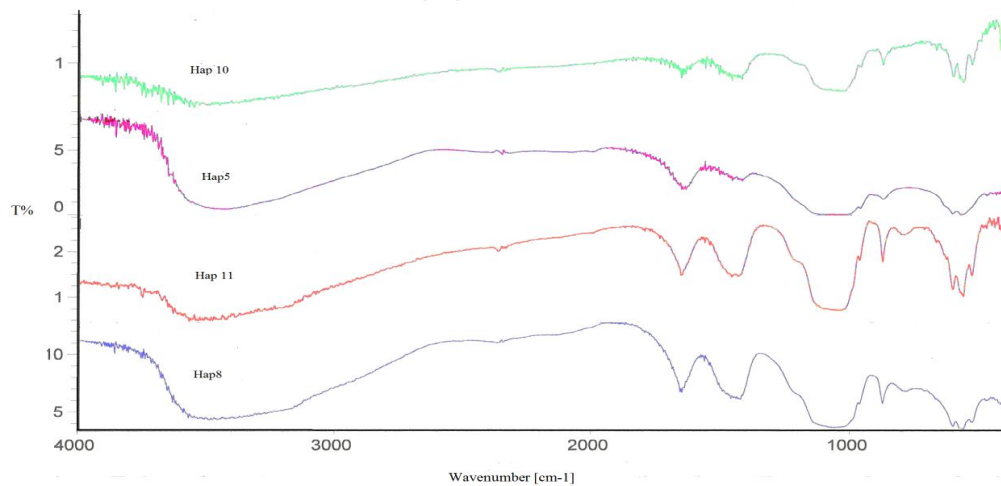These results confirm the results obtained by X-ray diffraction.

Figure 4: IR spectra analysis of the effect of time of microwave activation on nanocrystalline apatites
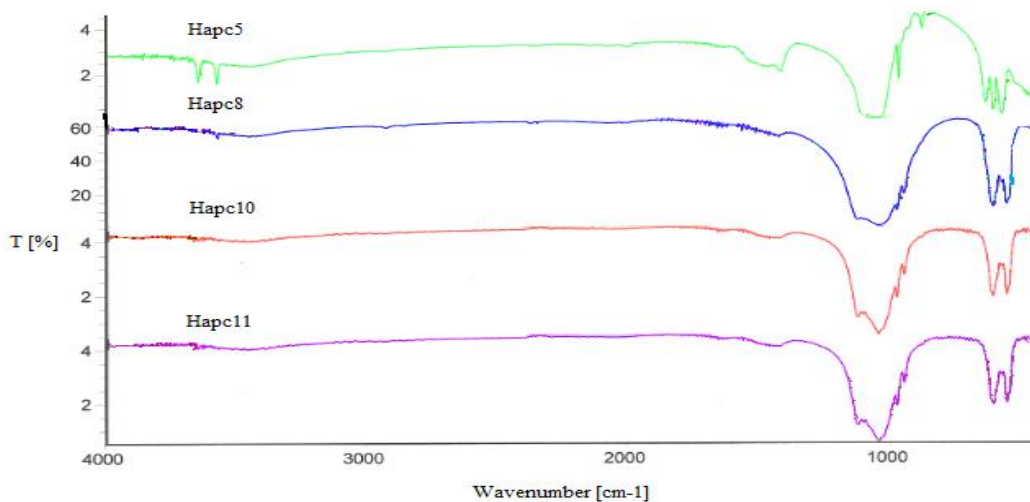

Figure 5: IR spectra analysis of the effect of calcination on nanocrystalline apatites

Comparing the results obtained in this work we observe formation of two man of biomaterials using the only one synthesis just with changing time of activation the synthesis by microwave:
ACP, CDHA and finally after calcination CDHA and β TCP.
After activation of synthesis the first 5 minutes, there is formation of ACP which transforms to carbonated CDHA after calcination.
For the other samples Hapc8, Hapc10, Hapc11 we obtained carbonated CDHA that transforms in β TCP after calcinations. Perhaps, this difference is due in Ca/P ratio. Arnaud Destainville and coauthor's study allowed to highlight the high variability of the Ca/P ratio of the powders with the experimental conditions. In general it was observed an increase in this ratio with the maturation time. The kinetics of the hydrolysis reactions which take place during the synthesis may explain the rapidity of the increase in the Ca/P ratio at the beginning of the reaction. In accordance with a thermally activated reaction process, the temperature favors the hydrolysis reactions [43].
In order to evaluate the effect of hydrolysis on Ca/P ratio and of nature of phase, S. Somrani and coauthors **[50]** performed at three different liquid ratio samples. Because of the very low solubility of the Ca-P phases, the influence of the amount of ions in the solution on the Ca/P ratio of the solid phase depends strongly on the liquid-to-solid ratio. The increase (or decrease) of the solid Ca/P ratio is necessarily linked to a decrease (or increase) of that in the solution, to maintain the total composition constant. They found significant increase of the Ca/P ratio of the solid phase when the liquid/solid ratio becomes very high which could considerably affect the composition of the apatitic phase formed.

Based upon these concepts, we can explain why there is formation of ACP after the first 5 minutes of activation by microwave which transformed after calcinations on CDHA while for other microwave activation times are longer there is formation of CDHA enhanced by hydrolysis phenomenon and valorized by decrease of the solid liquid ratio which leads to a equilibrium and a decrease in the Ca/P ratio which is close to 1.5 inducing the formation of pure βTCP after calcination.

Comparing the results obtained in this work we observe formation of two kinds of biomaterials using the only one synthesis just with changing time of activation the synthesis by microwave:

ACP, CDHA and finally after calcination CDHA and β TCP.

3.3 *Thermogravimetric analysis :*

Thermal Decomposition

Figure 6 illustrates thermogravimetric analysis (TGA) measurement of sample synthesized taken at t = 5 min. The sample showed weight loss with increasing temperature. Total weight loss on heating from 25 to 800°C is evaluated to be about 11.6 %.

The FTIR spectra of as synthesized samples shown in figure 3 exhibit clear evidence of CDHA [Usually expressed as $Ca_{10-x}(PO_4)_{6-x}(HPO_4)_x(OH)_{2-x}.xH_2O$](the name is originate from loss of Ca^{2+} ions from the unit cell of hydroxyapatite). The HPO_4^{2-} formation results from occupation by H_2O molecules at the vacant OH^- sites and hydrogen bonding to the nearest PO_4^{3-} groups as:

$$PO_4^{3-} + H_2O \longrightarrow HPO_4^{2-} + OH^-$$
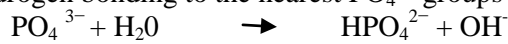
   i.   Between 25 and 200°C with the loss of 7,43 % :

TGA curves display a continuous mass loss with constant temperature increase. The water molecules adsorbed on the surface discharges were lost (temperature less than 250) [51].

   ii.   Between 220 and 470°C with the weight loss of 2,5 %:

Furthermore, this class of calcium phosphates absorbs much energy during microwave processing in relatively short times and has poor stability than stoichiometric HA. Under non-equilibrium conditions and lower stability a part of CDHA transform to $Ca_2P_2O_7$ [52] as given :

$$(1) \quad 2Ca^{2+} + 2HPO_4^{2-} \rightarrow Ca_2P_2O_7 + H_2O$$
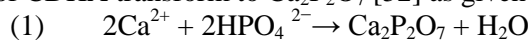
In our sample, a fast slop change is presented over 350 with a maximum at about 400°C in the derivative curve, indicating again a mass loss which can be due to the partial removal of physically and chemically adsorbed water.

   iii.   Between 470 and 620°C:

This range may be assigned to the transformation of amorphous $Ca_2P_2O_7$ to crystalline $Ca_2P_2O_7$

The peak observed at about 545°C, on derivative curve indicate that some structural reorganization occurs in this particular temperature range. This can be attributed to the condensation of hydrogenophosphate ions (HPO_4^{2-}).

A mass loss between the temperature range of 600-900°C possibly corresponds to the decarboxylation of the Hap, releasing CO_2 and the condensation of HPO_4^{2-} releasing water and possibly brings about elimination of interstitial water in crystal lattice [18,33] and the moisture discharged from pores up to 500°C as reported by Liga Berzina-Cimdina and Natalija Borodajenko [51].

At temperature below 750°C the agglutination begins, the results show that the CDHA (TCP) phase transformed into βTCP, according to the following equation 2 [51, 52, 53]:

$$(2) \quad Ca_9HPO_4(PO_4)_5OH \longrightarrow 3Ca_3(PO_4)_2 + H_2O$$
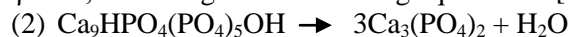
As reported by Thermal stability is characterized by decomposition temperature of Hap sample. The decomposition occurs when critical dehydratation point is achieved. In the temperature less than critical point, crystal structure of Hap remains inchanged in spite of stage of dehydratation. Achieving the critical point, complet irreversible dehydroxillation occurs, which results damage of Hap structure, decomposing onto tricalcium phosphate [18, 51].

In literature it is reported that CO_2 is discharged from the sample between $450 - 950$°C [51].

The carbonate bands and $P_2O_7^{4-}$ completely disappear after heating at 800°C, indicating that transformation of CDHA to βTCP is completed after this heat treatment. The other decomposition of CDHA taking place with loss of water by reaction 3:

$$(3) \quad P_2O_7^{4-} + 2OH^- \longrightarrow 2PO_4^{3-} + H_2O$$
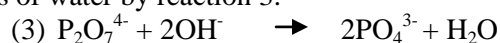
The nature of sample of t = 10 min is after calcinations is βTCP as reported in IR and DRX analysis.
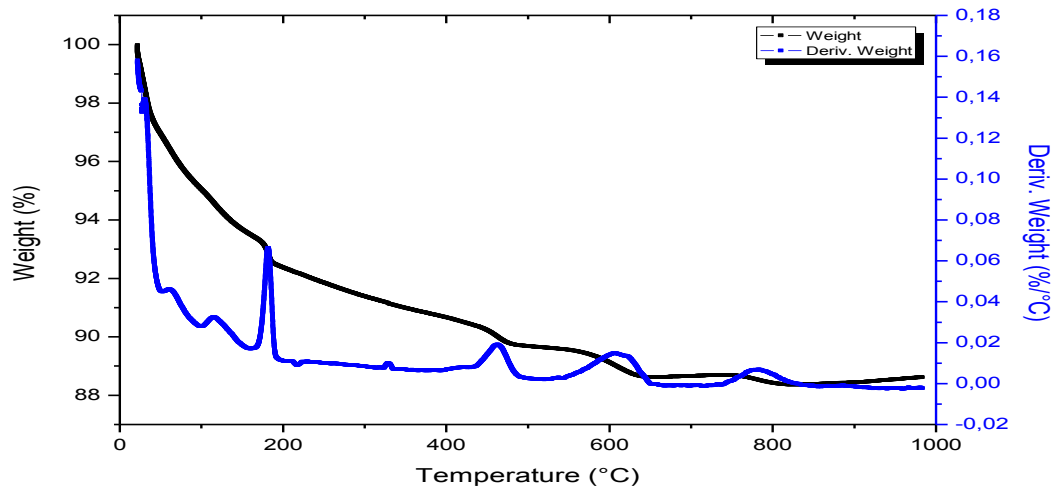
Figure 6: Thermogravimetric analysis of sample Hap10

3.4 *Morphology analysis:*

The size and morphology of fine powders are determined with TEM. The dark field transmission electron microscopic images of as synthesized and calcined samples are shown respectively **in figure 7. Almost** the particles are spheroid with different diameter corresponding of time of microwave activation and calcinations. The TEM images of the as synthesized powders revealed that the particles were predominantly agglomerated and that the individual particles appeared spherical.
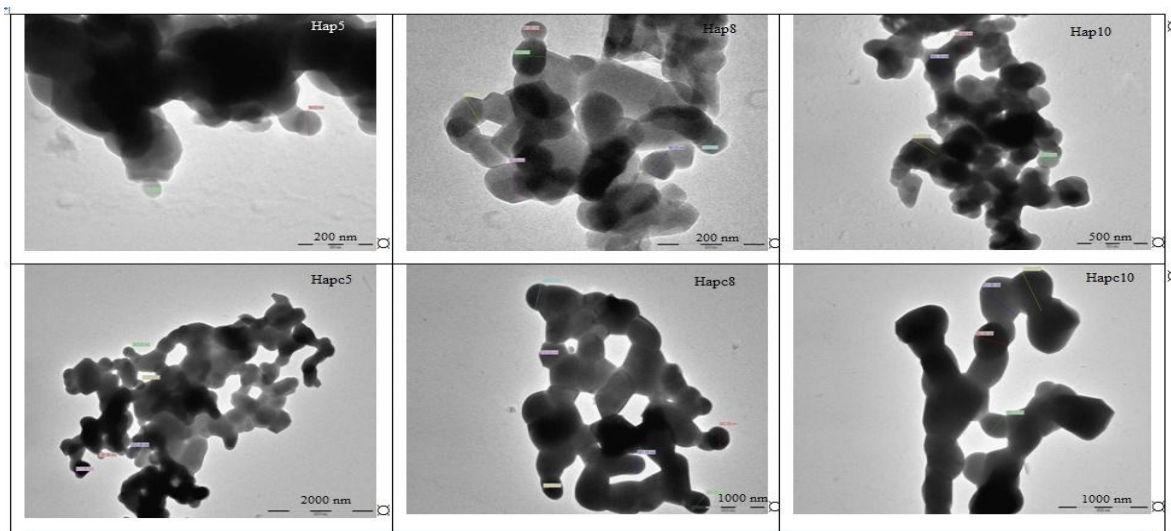

Figure 7: TEM image and electron diffraction pattern of samples as synthesized Hap5 and after calcinations at 900°C

However, it should be noted that the particles do not posses high regularity in shape; in other words, their surfaces are smooth. In addition, the particles show a high tendency towards agglomeration except for Hap5 sample who is almost amourphous with some particles with 60 nm in diameter.

A novel microwave process for synthesizing nanosize Btcp (Hapc5, Hapc8, Hapc10) with spherical shape was thus developed. In most report concerning the synthesis of β-TCP, the particles shapes are plat [51] or polyhedra [54], but nanoparticles with spheroidal morphology were successfully prepared in the current research. Because the spherical geometry rather than irregular shape is important for achieving osteointegration [55-56], the products synthesized via microwave process are preferred for medical applications. However, it was confirmed using TEM that the microwave prepared powders have nanocrystalline structures with appropriate morphology.

Thus we determined that, after 5, 8, 10 and 11 minutes of the synthesise in microwave and subsequent thermal treatment at 900°C, this method rise to pure β-TCP with average sizes are different and depend of microwave activation time and with calcination as reported in table 3.

Table3: particles size of powders as synthesized and after calcination

Samples as synthesized (Fig.6)	Hap5	Hap8	Hap10
Average diameter (nm)	amorphous	60 ±10	180 ± 20
Samples after calcinations (Fig.7)	Hapc5	Hapc8	Hapc10
Average diameter (nm)	200 ±20	320 ±20	500 ± 20

Conclusion

We used the method of microwave as a source of heat input for synthesis. This method has some advantages such as heating throughout the media, rapid heating, fast reaction, high yield, excellent reproducibility, narrow particle distribution, high purity and high efficient energy transformation , and being environmentally cleaner. A simple, high yield process involving inexpensive reagents, no control of pH has been set up for production tree kinds of calcium phosphates.

There is formation of CDHA as an intermediate product pholphocalcique of ACP. After calcination at 900°C the CDHA transformed to pure nanocrystalline β tricalcium phosphate which is also used as biomaterial.

It has been inferred that the structure of the synthesized product is related to time of activating by microwave synthesis and heat treatment after synthesis (effect of calcination).

Thermal transformation of CDHA involved the dehydroxylation, decarboxylation and phosphate decomposition and decarbonatatin.

The nanometric grain size of Ca-P changed to the size with time of microwave activation and after calcinations.

References:

1. Gopal S. N., Zheng P. Y., Lin L., Bin H. Ch. *Nanomedicine* 8(4)(2013) 639-653

2. Nathanael A.J., Seo. TH Oh., N*anomater (2015)* 1-9

3. Bohner M. , Tadier S. , Van Garderen N. , De Gasparo A. Döbelin N. and Baroud G. , *Biomatter.* 3(2)(2013) 1-15

4. Sheikh Z., Brooks P. J., Barzilay O., Fine N., Glogauer M., *Mater.* (8) (2015) 5671-5701

5. Gandou Z., Nounah A., Belhorma B., Yahyaoui A., *J. Mater. Environ. Sci.,* 6 (4) (2015) 983-988.

6. Nag S. and Banerjee R. , *ASM handbook, Volume 23 :Materials for Medical Devices* 23 (2012) 6-17

7. Dorozhkin Sergey S. V., *Pro. Biomat.* (1)(2012) 1-40

8. LeGeros R. Clin. Z. *Orthop. Relat. Res*. 395(2002) 81-98

9. Drouet C., Bosc C., Banu F., Largeot M., Combes C., Dechambre C., Estournès G., Raimbeaux C. G. and Rey C., *Powder Technol.* 190 (2009)118- 122.

10. Wua S.C., Hsua H.C., Hsua S.K., Chang Y.C. b, Hoc W-F, *Journal of Asian Ceramic Societies* 4 (2016) 85– 90

11. Destainville A. Thesis (2005) 11-38

12. Roveri N., Iafisco M. chap. 4, "Advances in biomimetic", *Biomed. Eng.* (2011)75-102

13. Webster T.J, Ergun C., Doremus R. H., Siegel R. W, Bizios R., *Biomaterials* 21(2000)1803-1810

14. Bauer L. A., Birenbaum N. S., Meyer G. J., *J. Mater. Chem*. 14(2004)517-526.

15. Keck W. M., *J. Am. Ceram. Soc.* 92 (11) (2009) 2528-2536.

16. Sergey V. Dorozhkin, "Calcium Orthophosphates: Applications in Nature, Biology, and Medicine" Book by *Pan Stanford Publishing* 2012.

17. Sadat-S. M., Taghi Khorasani M., Dinpanah-Khoshdargi E., Jamshidi A. *Acta Biomater.* 9 (2013) 7591– 7621.

18. Meejoo S., Maneeprakorn W., Winotai P., *Thermochim. Acta* 447 (2006) 115–120.

19. Lee B.T., Youn M.H., Rajat K. Paul R.K., Lee K.H,. Song. H.Y, *Mater. Chem. Phys.* 104(2007) 249–253.
20. Khan N.I., Ijaz K., Zahid M., Khan A.S., Abdul Kadir M.R., Hussain R., Anis-U., Darr JA, Ihtesham-U., Chaudhry A.A., *Mater Sci . Eng C Mater Biol Appl. Nov 1(56)((*2015) 286-93.
21. Ramli R**.**, Zafirah A. Arawi O., Kumar T. M., Mahat M. M., Umi S., Jais U.S., *AIP Conference Proceedings*; Vol. 14555(1) (2012)45
22. Bramhe S., Ryu J.-K., Chu1 M. C., Balakrishnan A. and Kim T. N., *Korean J. Mater. Res*. 24(2014)700-703.
23. Vani. R, Raja S.B., Sridevi T., Savithri K., Devaraj S.N., Girija E., *Nanotechnology* 22(2011)285701 [10p].
24. Rameshbabu N., Rao KP, Kumar TSS. *J. Mater. Sci.* 40 (2005)6319–6323.
25. Torrent-Burgues J., Gomez-Morales J., Lopez-Macipe A., Rodriguez-Clemente R., *Cryst. Res. Technol.* 34 (1999)757–762.
26. Wang K.W., Zhu Y.-J, Chen, Cheng G.-F., Huang Y.-H. *Mater. Lett*. 65 (2011) 2361–2363.
27. Poinern G.E.J., Brundavanam R., tho X. Le , Djordievic S., Provic M. Fawcett D., *Int. J. of Nanomed. (09/2011) 2083-2095.*
28. Jalota S., Tas AC, Bhaduri SB. *J. Mater. Res.* 19(2004)1876–1881.
29. Liang T., Qian J., Yuan Y., Liu C., *J.Mater. Sci.* 48, 15 (2013) 5334-534.
30. Nazir R., Khan A., Aftab A., Ur-Rehman A., Chaudhry A. A., UrRehman I., Wonge F.L. *Ceram. Int.* 39 (2013) 4339–4347.
31. Nazir R., Iqbal N., Abdul S., Khan A. S Aftab A. Anila A. Aqif A. Chaudhry A., Ihteshamur. Rehman, Rafasat H. *Ceram. Int.* 38(2012) 457-462.
32. Sha L., Liu Y., Zhang Q., Hu M., Jiang Y., *Mater. Chem. Phys.* 129 (2011) 1138– 1141
33. Kalita S. J., Verma S., *Mater. sci. Eng.* C 30 (2010) 295-303
34. Arami H., Mohajerani M., Mazloumi M., Khalifehzadeh R., Lak A., Sadrnezhaad S.K., *J. Alloys and Compd* 469 (2009) 391.
35. Siddharthan A., Seshadri S. K. and Sampath Kumar T. S. *Trends Biomater. Artif. Organs* 18(2)(2005)110-113
36. Wang Y.Z., Fu Y. *Mater Lett*. 65 (2011)3388-3390.
37. Ramli R., Omar Arawi A. Z., Talari M. K., Mahat M. M., Unmi Sarah Jais R., *American Institute of Physics* 2012 2nd ASEAN – APTCTP Workshop
38. Rameshbabu N., Prasad Rao K., *Curr. Appl Phys*., 9 (2009) S29–S31.
39. Sampath Kumar T.S. Manjubala I., Gunasekaran J. *Biomaterials* 21 (2000) 1623-1629.
40. Pasand E**.**G, Nemati A. Solati Hashjin M., Arzani K. Farzadi A., *Int J Min Met Mater* 19 (2012) 441-445
41. Aminian A., Solati-Hashjin M., Samadikuchaksaraei A., Bakhshi F., Gorjipour F., Farzadi A., Moztarzadeh F., Schmucker M. *Ceram. Int.* 37 (2011) 1219–1229.
42. Byong-Taek L., Min-Ho Y. , Rajat Kanti P. , Kap-Ho L. , Ho-Yeon S., *Mater. Chem. Phys.,* 104 (2007) 249–253.
43. Destainville A. Champion E., Bernach-Assolant D. *Mater. Chem. Phys. 80* (2003) *269-277.*
44. Ratner B., Hoffman A., Shoen F. *Biomaterials Scienc*. (2004) 851.
45. Mortier A., Lemaître J., Rodrique L. and Rouxhet P. G, *J. Solid State Chem*. 78 (1989) 215
46. Andres-Verges M., Gonzalez F. and Gallego M., *J. Eur. Ceram. Soc.,* 18 (1998) 1245.
47. Koutsopoulos S., *J. Biomed. Mater. Res.* 62 (2002] 600
48. Wilson R. M., Elliot J. C., and Dowker S. E. P., *J. Solid State Chem*. 174 (2003) 132
49. Zyman Z.Z., Tkachenko M.V., Polevodin D.V., *J. Mater. Sci. Mater. Med.*, 19 (2008) 2819-2825.
50. Somrani S., Banu M., Jemal M., Rey C., *J. solid State chem.* 178 (2005) 1337-1348
51. Berzina-Cimdina L. Borodajenko N., *Intech*, (2012)123-148
52. Lazic S., *J. Cryst. Growth* , 147 (1995) 147–154
53. Dasgupta S., Tarafder S., Bandyopadhyay A., Bose S., *Mater. Sci. Eng.* C, 33 (2013) 2846-2854.
54. Sergey V. Dorozhkin *Materials 2 (*2009) 1975-2045.
55. Hsu, Y. Turner, I.G., & Milles, A. W., *J. Mater. Sci. : Mater Med.*, 18 (2007) 1931-1937.
56. Nayar, S., Sinha, M. K., Basu D., Sinha, *J. Mater Sci: Mater Med.*, 17 (2006) 1063-1068.